Mechanics of curved surfaces, with application to surface-parallel cracks

Stephen J. Martel[1]

Received 19 August 2011; revised 14 September 2011; accepted 16 September 2011; published 20 October 2011.

[1] The surfaces of many bodies are weakened by shallow enigmatic cracks that parallel the surface. A re-formulation of the static equilibrium equations in a curvilinear reference frame shows that a tension perpendicular to a traction-free surface can arise at shallow depths even under the influence of gravity. This condition occurs if $\sigma_{11}k_1 + \sigma_{22}k_2 > \rho g \cos\beta$, where k_1 and k_2 are the principal curvatures (negative if convex) at the surface, σ_{11} and σ_{22} are tensile (positive) or compressive (negative) stresses parallel to the respective principal curvature arcs, ρ is material density, g is gravitational acceleration, and β is the surface slope. The curvature terms do not appear in equilibrium equations in a Cartesian reference frame. Compression parallel to a convex surface thus can cause subsurface cracks to open. A quantitative test of the relationship above accounts for where sheeting joints (prominent shallow surface-parallel fractures in rock) are abundant and for where they are scarce or absent in the varied topography of Yosemite National Park, resolving key aspects of a classic problem in geology: the formation of sheeting joints. Moreover, since the equilibrium equations are independent of rheology, the relationship above can be applied to delamination or spalling caused by surface-parallel cracks in many materials. **Citation:** Martel, S. J. (2011), Mechanics of curved surfaces, with application to surface-parallel cracks, *Geophys. Res. Lett.*, *38*, L20303, doi:10.1029/2011GL049354.

1. Introduction

[2] This paper examines a fundamental yet under-appreciated role that curvature plays in the mechanics of surfaces. Where coupled with high compressive stresses parallel to a surface, the influence of surface curvature can alter the near-surface stresses profoundly and lead to fracturing. Fractures in turn weaken materials, create new surfaces upon which a broad array of physical, chemical, and biologic phenomena can occur, and provide pathways between the surface of a body and its interior. The findings here should be of broad use.

[3] Shallow fractures parallel to the boundaries of bodies are widespread. They occur over a broad range of scale ($<10^{-3}$ m -10^{2} m) and open in bodies as diverse as laminates and coated engineering materials [*He et al.*, 1998] and rock [*Matthes*, 1930]. The largest and most spectacular of these opening-mode fractures are called sheeting joints (or exfoliation joints) by geologists. These fractures help define iconic landmarks such as Half Dome in Yosemite Valley, California (Figure 1) and are discussed in nearly every introductory physical geology class. Some sheeting joints extend for more than 100 m laterally [*Bahat et al.*, 1999] and open at depths of 100 m or more [*Jahns*, 1943]. Sheeting joints strongly influence landscape development [*Bradley*, 1963], groundwater systems [*LeGrand*, 1949; *Trainer*, 1988; *Borchers*, 1996], and slope stability [*Terzaghi*, 1962; *Hermanns and Strecker*, 1999; *Wieczorek and Snyder*, 1999; *Chigira*, 2001]. They also are associated with bursting rock in mines and quarries [*Niles*, 1871; *Twidale*, 1973; *Twidale and Bourne*, 2000]. In spite of numerous studies beginning more than two centuries ago [*Dale*, 1923], however, the root cause of sheeting joints has remained elusive.

[4] Certain characteristics of sheeting joints distinguish them from other opening-mode fractures in rock. They are distinctly curved and develop best beneath domes [*Gilbert*, 1904], topographic surfaces that are convex in two perpendicular directions tangent to the surface. They form where high compressive stresses parallel the ground surface [*Holzhausen*, 1977, 1989]. How these characteristics are related has been enigmatic.

[5] Although sheeting joints are widely considered as "unloading fractures", caused by erosion of overburden [e.g., *Thornbury*, 1954], this scenario is inconsistent with four key observations. First, some sheeting joints occur in rocks that were never deeply buried [*Bradley*, 1963; *Holzhausen*, 1989]. Second, they are absent in many rocks exhumed from great depths [*Vidal Romaní and Twidale*, 1999]. Third, sheeting joints do not form in dimension stone, which is "completely unloaded" after extraction from quarries, or in talus. Fourth, in exhumed granitic terranes with sheeting joints, the joints typically are scarce in valleys, where overburden erosion is locally greatest, but are relatively abundant on the flanking convex mountains and ridges, where overburden erosion is locally least.

[6] A viable physical mechanism for sheeting joints must explain how they open. New fractures tens of meters long do not open simply in response to the elastic rebound (strain) of a body that accompanies unloading of its surface. Opening of new macroscopic fractures instead requires either a tensile stress or a localized fluid pressure that exceeds the ambient least compressive stress [*Nemat-Nasser and Horii*, 1982; *Pollard and Segall*, 1987]. Intrinsic residual stresses can be ruled out because sheeting joints do not develop in dimension stone. Settings with sheeting joints typically lack a mechanism for generating high fluid overpressures, and the joints characteristically lack minerals precipitated from high-pressure fluids. This leads to an apparent paradox: sheeting joints require a tension perpendicular to the ground surface at shallow depths, yet the surface itself sustains no such tension, and gravity increases the vertical compressive stress with depth.

[1]Department of Geology and Geophysics, University of Hawaii, Honolulu, Hawaii, USA.

0094-8276/11/2011GL049354

Figure 1. Sheeting joints near the summit of Half Dome, Yosemite National Park. They bound shingle-like slabs that are on the order of 1 m thick. Photograph courtesy of Greg Stock.

[7] In this manuscript I present and test a new physically based hypothesis for the formation of sheeting joints that resolves this apparent paradox. The starting point involves reconsidering how the tension normal to the ground surface (T) could vary as a function of depth normal to the surface (z). This function is usually considered to have a negative slope (Figure 2, dashed curve). If, however, its slope is positive at the surface, where $z = 0$ (Figure 2, solid curve), then a tension must arise in the shallow subsurface. I present a fundamental solution for the slope of the T vs. z curve at the ground surface as a function of three quantities: (a) the compressive stresses parallel to the surface, (b) the surface shape, and (c) gravitational stresses. This slope (derivative) can be positive, yielding a tensile stress perpendicular to the surface at shallow depths, if the compressive stresses parallel to the surface are sufficiently strong and the surface is sufficiently convex in at least one direction. The hypothesis is that this condition promotes the opening of sheeting joints. I then test the hypothesis against spatial patterns of sheeting joints in the field and then close by noting a few of the many other applications of the mechanism presented here.

2. Mechanics

[8] A free body diagram for a thin element bounded by a convex traction-free upper surface illustrates the essential physics of the proposed mechanism (Figure 3a). This element could be considered as part of the "skin" of a rock outcrop. Compressive (negative) stresses acting parallel to the convex surface yield a net outward radial force on the element. If this overcomes the inwardly directed net force due to gravity and the tensile strength of the material at the base of the element, then the element will not remain in equilibrium and would separate from its substrate. In a rock mass, tensile failure at the element base would produce sheeting joints.

[9] The approach here extends a previous solution for idealized cylindrical surfaces [*Martel*, 2006] to surfaces of arbitrary shape using a local reference frame based on orthogonal curvilinear coordinates. According to principles of differential geometry [*Gauss*, 2005] the directions of the maximum and minimum normal curvatures at a point on a surface are orthogonal (Figure 3b). The orthogonal reference frame directions α_1, α_2, and α_3 parallel the direction of the most concave (most positive) principal curvature (k_1), the most convex (most negative) principal curvature (k_2), and the outward normal to the surface, respectively (Figure 3b). Along the surface, $\alpha_3 = 0$. The z-direction is the inward normal to the surface. The stress component σ_{ij} acts on a face with an outward normal in the i-direction and acts in the j-direction, so σ_{11}, σ_{22}, and σ_{33} act in the directions of α_1, α_2, and α_3, respectively. Tensile stresses are considered positive. Note that σ_{33} in Figure 3b equals T in Figures 2 and 3a.

[10] The equation of static equilibrium relates the stresses and body forces acting on or in a body of any rheology. Static equilibrium exists in a continuous medium if the divergence of the stress tensor σ and the body force vector $\boldsymbol{F}$ at each and every point sum to zero [*Malvern*, 1969]:

$$(\nabla \bullet \sigma) + F = 0. \tag{1}$$

The divergence of σ (i.e., $\nabla \bullet \sigma$) and $\boldsymbol{F}$ are vectors with three orthogonal components. The key components here act in the α_3-direction. The general expression for $(\nabla \bullet \sigma)_3$ is somewhat complicated [*Malvern*, 1969] but simplifies greatly at a traction-free surface (i.e., $\alpha_3 = 0$) using the reference frame introduced here (see auxiliary material for the full derivation):[1]

$$(\nabla \bullet \sigma_3)|_{a_3=0} = \frac{\partial \sigma_{33}}{\partial \alpha_3} + \sigma_{11}k_1 + \sigma_{22}k_2, \tag{2}$$

where the principal curvatures k_1 and k_2 are positive where concave and negative where convex. The other factor on the left side of equation (1) is the body force vector $\boldsymbol{F}$, assumed here to be exclusively due to gravity. Following Figure 3a, its component normal to the surface is

$$F_3 = -\rho g \cos\beta, \tag{3}$$

where ρ is the rock density, g is gravitational acceleration, and β is the slope of the surface. Substituting (2) and (3) into (1) yields a simple force balance expression at the surface:

$$\left(\left. \frac{\partial \sigma_{33}}{\partial \alpha_3} \right|_{\alpha_3=0} + \sigma_{11}k_1 + \sigma_{22}k_2 \right) - \rho g \cos\beta = 0. \tag{4}$$

Recasting (4) in terms of the z-direction rather than the α_3-direction and replacing σ_{33} by T yields the slope of the tension vs. depth curve at the topographic surface in Figure 2, here called ϕ:

$$\left. \frac{\partial T}{\partial z} \right|_{z=0} = \phi = \sigma_{11}k_1 + \sigma_{22}k_2 - \rho g \cos\beta. \tag{5}$$

In other words, equation (5) gives the normal traction gradient at the surface.

[11] If ϕ is positive, then a tension perpendicular to the surface will exist at shallow depths (the scale for evaluating depth is discussed subsequently). Rocks are so weak in tension that in engineering design they have been considered to have no long-term tensile strength [*Bazant*, 1996]. As a result, sheeting joints can be expected to nucleate beneath slopes where the sum of the two stress-curvature products on the right side of equation (6) exceeds the

[1] Auxiliary materials are available in the HTML. doi:10.1029/2011GL049354.

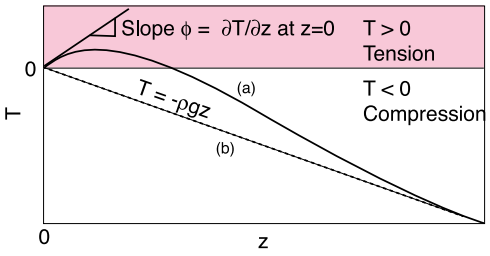

Figure 2. Two curves showing tension normal to a traction-free surface (T) as a function of normal distance (z) below the surface. Solid curve (a) shows tensile stresses at a shallow depth and has a positive slope at $z = 0$. Dashed curve (b) shows stresses becoming progressively more compressive with depth and has a constant negative slope.

product of the unit weight of rock (ρg), ~2.6×10^4 Pa·m^{-1} for many crystalline rocks, and the cosine of the slope. In other words, $\phi > 0$ is a necessary criterion for the formation of macroscopic sheeting joints.

[12] A qualitative review of equation (5) sheds light on sheeting joints. If surface curvatures are sufficiently convex (negative) and surface-parallel stresses sufficiently compressive (negative), then their products could be sufficiently positive to promote sheeting joints. This is consistent with the common occurrence of sheeting joints in domes and ridges in regions with high surface-parallel compressive stresses. On the other hand, if surface curvatures are concave (positive) and surface-parallel stresses are compressive (negative), then their products are negative. This is consistent with the scarcity of sheeting joints in bowls and valleys. Perfectly planar surfaces are rare in nature but also would yield negative values of ϕ and would not be expected to serve as nucleation sites for macroscopic sheeting joints. Saddles, surfaces that are concave in one direction and convex in another, that experience surface-parallel compressive stresses will have stress-curvature products of opposing signs. Sheeting joint nucleation could be either promoted or retarded beneath saddles depending on the magnitudes of the stress-curvature products.

3. Analysis and Results

[13] An area near Olmsted Point in Yosemite National Park, California (Figure 4a) was selected for four key reasons to test the hypothesis that surface-parallel stresses and topography account for the opening of sheeting joints. First, it hosts a spectrum of topographic shapes. Second, it contains expanses of glacially scoured granitic bedrock where sheeting joints are abundant in some areas and scarce in others. Third, the stresses at the surface have been evaluated nearby, 15 km to the east-northeast in Tuolumne Meadows, from overcoring measurements [*Cadman*, 1970]. The most compressive stress obtained was −14 to −21 MPa at a bearing of 30°, with a least compressive stress of −6.5 to −11 MPa at a bearing of 120°. The minus signs denote compressive stresses. Fourth, many sheeting joints there are geologically young, having formed in the last 10,000–20,000 years since the area was swept by glaciers [*Gillespie and Zehfuss*, 2004], as evidenced by the many loose joint-bounded rock slabs that now litter glaciated surfaces. Among the youngest is a sheeting joint that formed in the last 60 years in a road cut 0.4 km NE of Olmsted Point (see auxiliary material). Accordingly, the current topography and the current stress field should reflect the conditions during the formation of many sheeting joints.

[14] Digital topographic data near Olmsted Point were collected by the National Center for Airborne Laser Mapping (NCALM) and permit calculation of the surface curvatures and slopes. These laser altimetry (LIDAR) data are now freely available from NCALM. Data were collected at a nominal point spacing of 1 m, interpolated onto a 1 m square grid, and filtered [*Perron et al.*, 2008] to remove

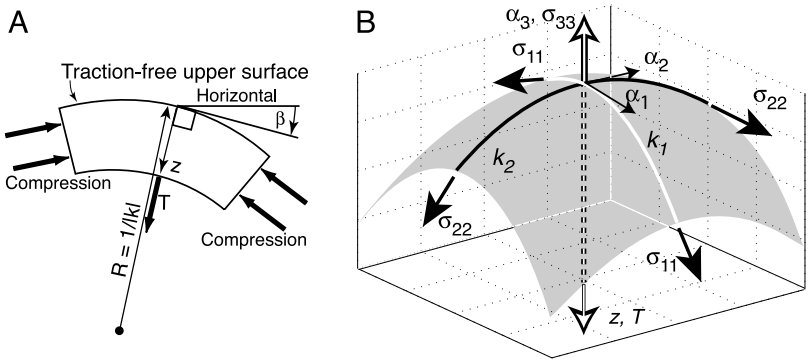

Figure 3. Notation for reference frames and stresses at a curved surface. (a) Cross section showing compressive (negative) stresses (unlabeled bold arrows) parallel to a thin concave element of a traction-free surface with a tensile (positive) stress (T) at the base of the element. The term z is the depth normal to the surface, R is the radius of curvature of the surface, and β is the slope of the surface. (b) Curvilinear local reference frame with its origin at the surface of a convex body. The orthogonal reference frame axes are aligned along directions of the principal curvatures. The α_3-direction is the outward normal to the surface and along the intersection of two perpendicular planes. These planes intersect the surface at two locally perpendicular circular arcs (heavy curves). The tangents to these arcs define the directions α_1 and α_2, with α_1 along the most concave (or least convex) arc (white), and α_2 along the most convex arc (black). The corresponding reciprocals of the radii of these arcs are the principal curvatures k_1 and k_2. The normal stresses σ_{11}, σ_{22}, and σ_{33} (heavy arrows) act parallel to α_1, α_2, and α_3, respectively. Tensile (positive) stresses are shown.

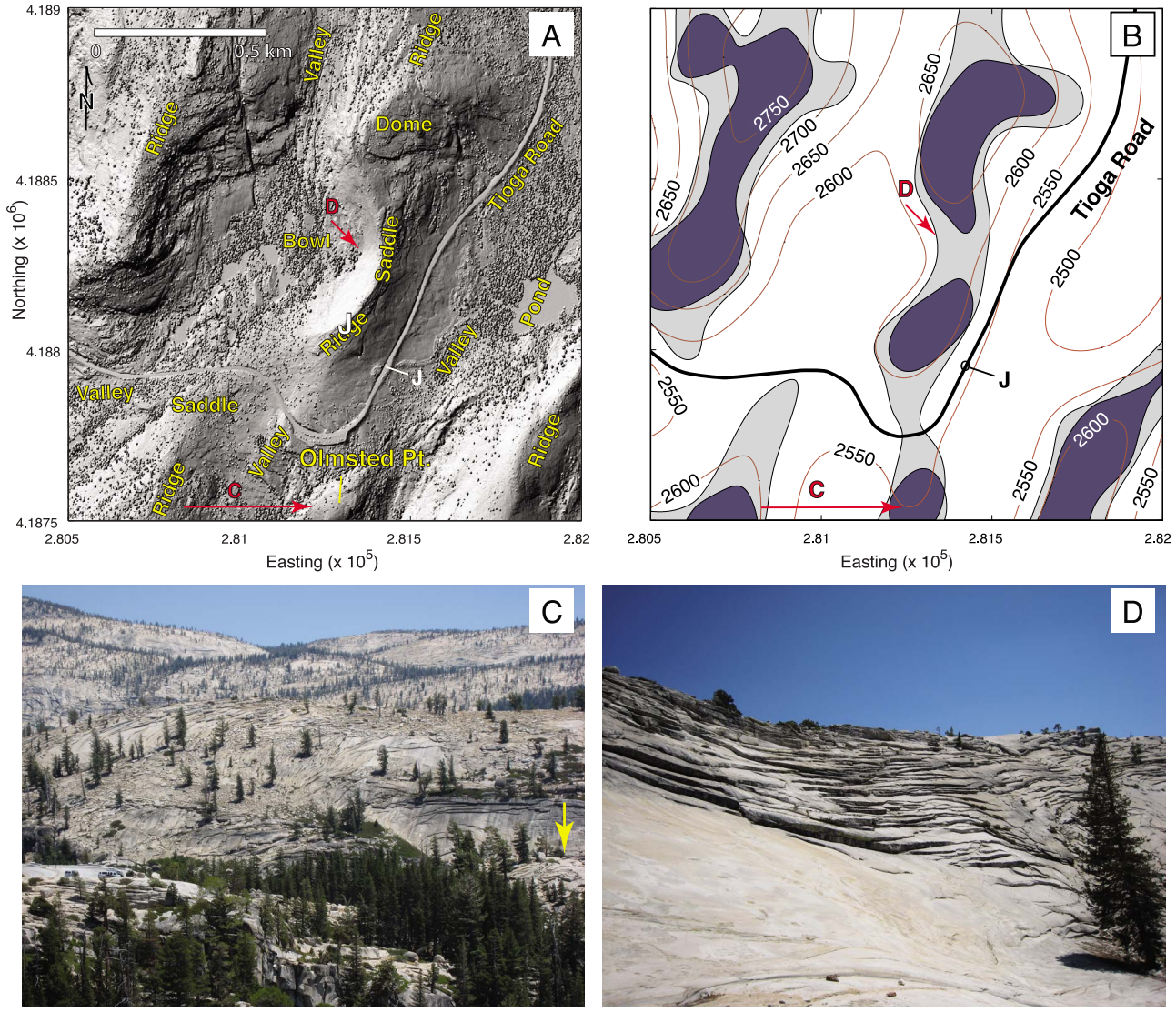

Figure 4. Locations of topographic features, predictions of sheeting joints, and occurrences of sheeting joints near Olmsted Point, Yosemite National Park. (a) Shaded relief image from LIDAR data. Illumination is from the west. The topographic grain trends north-northeast, so west-facing slopes are bright and east-facing slopes are dark. Red arrows mark directions of Figures 4c and 4d. Feature J is a sheeting joint formed historically at a road cut along the Tioga Road. Universal Transverse Mercator (UTM) coordinates are in meters for zone 11, using the 1983 North American Datum (NAD83). (b) Regions where sheeting joints are predicted to occur (blue), are predicted to not occur (white), and that are indeterminate (gray), assuming that $\sigma_2 = -14$ MPa and $\sigma_1 = -6.5$ MPa. The brown contour lines have a 50 m contour interval. (c) Photograph looking east across the southern portion of the study area. Sheeting joints decorate virtually every exposure in this picture. Olmsted Point (arrow) is at the right edge of the picture, with the Tioga Road at the left. The ridge at the southeast corner of Figure 4a is in the middle ground. (d) Photograph looking southeast at the slope 0.7 km north of Olmsted Point. Sheeting joints are abundant in the saddle-shaped upper part of the picture but scarce in the bowl-shaped lower portion.

features with wavelengths less than 200 m while retaining the major features in the landscape. The auxiliary material describes the data and reduction procedures in detail and provide computer codes for calculating the curvatures and slopes.

[15] In the analysis here, the magnitudes of the principal stresses at Tuolumne Meadows are applied to the entire Olmsted Point area. This simplification introduces errors arising from both extrapolation and neglect of topographic perturbations of the stress field [*Savage and Swolfs*, 1986] but seems reasonable in light of shallow hydraulic fracturing measurements ~45 km to the southeast that yield similar values [*Hickman et al.*, 1993]. Even if the magnitudes of the principal stresses at the surface vary little, however, their orientations must vary because of topography. To account for this, at least partially, the stress-curvature products are bracketed rather than calculated directly. The maximum value of σ_{11} or σ_{22} in equation (5) is σ_1, the most tensile stress, and the minimum value is σ_2, the least tensile stress. Accordingly, the quantity $\phi_A = \sigma_1 k_1 + \sigma_2 k_2 - \rho g \cos \beta$ serves as an upper bound for ϕ, and $\phi_B = \sigma_1 k_2 + \sigma_2 k_1 - \rho g \cos \beta$ as a lower bound for ϕ.

[16] Figure 4b shows where sheeting joints are predicted to occur (blue areas, $\phi_A > \phi_B > 0$) and are predicted not to occur (white areas, $0 > \phi_A > \phi_B$) near Olmsted Point. The gray areas, where $\phi_A \geq 0 \geq \phi_B$, are where the predictions are indefinite. Figure 4b was prepared assuming that $\sigma_2 = -14$ MPa and $\sigma_1 = -6.5$ MPa, but the results are nearly the same for $\sigma_2 = -21$ MPa and $\sigma_1 = -11$ MPa (the blues areas are slightly larger at the expense of the gray areas). Sheeting joints indeed are abundant in the blue areas (e.g., Figure 4c), which include all the major domes and ridges, as well as some saddles. Sheeting joints also are quite common in most of the gray areas, which include some ridges and several saddles. The white areas mark bowls, valleys, some saddles, and flat areas, many of which contain ponds or vegetation that conceal the bedrock. In the large granitic exposures of (a) the bowl north of Olmsted Point (Figure 4d), (b) the valley northeast of Olmsted Point and below the Tioga Road, and (c) the valley 0.2 km west of Olmsted Point, however, sheeting joints indeed are quite scarce. The sheeting joints that do occur in the white areas are found either in road cuts or at short-wavelength domes, ridges, or saddles, features that have been filtered out of Figure 4. The observations thus are consistent with the hypothesis that surface-parallel stresses and topography account for the opening of sheeting joints and are inconsistent with the "relief-of-overburden" hypothesis.

4. Discussion

[17] Equation (5) spotlights the key mechanical parameters responsible for sheeting joints. It redirects attention from sources of surface-normal tension to sources of surface-parallel compression. It shows that curvature and slope, rather than relief, are the key geometric parameters for the formation of sheeting joints. Rock type is important primarily in terms of its unconfined compressive strength and its density. Ironically, granite is susceptible to sheeting joints (tensile fractures) because of its ability to sustain high compressive stresses. In the context of equation (5), erosion of overburden promotes sheeting joints by the creation of curvature. If erosion just lowered the ground surface without generating curvature a few orders of magnitude greater than the value for the Earth as a whole, then sheeting joints would not be able to open.

[18] Equation (5) uses local information on (a) the stresses acting *parallel* to the boundary of a body and (b) the local surface shape to determine (c) how one stress component will change with distance from the boundary. Equation (5) is not the complete solution for a boundary value problem in mechanics (i.e., it does not fully determine the stress state in a body, or in any part of it, based on tractions or displacements acting *on* the boundary). Instead, the critical quantity $\partial T/\partial z|_{z=0}$ that equation (5) does determine depends solely on equilibrium considerations and hence is independent of rheology; this means the result applies to a broad range of materials.

[19] Equation (5) predicts the sign of T for distances beneath a surface that are small relative to the principal radii of surface curvature R_1 (= $1/|k_1|$) and R_2 (= $1/|k_2|$). This is because they are the only length scales in equation (5), albeit implicit. In the cases considered here, the radii of curvature are on the order of 1000 m, meaning that the results do apply to the depth range of several tens of meters at which sheeting joints typically occur. Other factors being equal, the depth to which this curvature-induced tension can penetrate will increase as the surface curvature decreases. Sheeting joints beneath broad, gently curved surfaces would therefore tend to extend to greater depths than those beneath small highly curved bumps.

5. Implications

[20] Some other implications of the solution merit mention here. First, the results here establish a way to link regional (tectonic) stresses and local fracture process at the Earth's topographic surface. Second, if sheeting joints occur where the topography is known but the surficial stresses are not, such as on another planet, the stresses could be estimated using equation (5) instead of requiring stress measurements. Third, for rock slopes that approach vertical, the cosine term on the right side of equation (5) approaches zero, and the surface-parallel stresses generally are compressive. In light of equation (5), steep slopes with a convex profile are likely to experience tensile stresses normal to the slope at shallow depth and are prone to develop fractures parallel to the slope surface. Such fractures, which can severely weaken slopes, typically would be concealed. Fourth, because the thin shells bounded by sheeting joints are prone to buckle and crack, sites with sheeting joints are likely to develop well-connected, hydraulically-conductive networks. Fifth, equation (5) can test analytical and numerical solutions of stresses near traction-free surfaces. Sixth, the results bear on delamination of engineering materials and coatings on curved surfaces under lateral compressive loads imposed by external loads or thermal stresses. The results also should bear on the physical weathering of rocks by spheroidal weathering.

6. Conclusions

[21] The effect of topography on stresses near a traction-free surface can be profound. The equations of equilibrium show that compressive (negative) stresses parallel to a convex traction-free surface will cause a near-surface tensile stress normal to the surface if the sum of the products of the principal curvatures and the associated compressive or tensile stresses parallel to the surface exceeds the product of the unit weight of the material and the cosine of the slope. This mechanism contributes fundamentally to sheeting joint formation in rock. Even slopes that appear flat to the unaided eye can possess sufficient curvature to cause tensile stresses to develop normal to the surface where lateral compressive stresses are high. The physical principles developed here are not restricted to rocks; they also provide insight into why other materials delaminate or spall when surface-parallel compressive stresses become high.

[22] **Acknowledgments.** This research has been supported by NSF (grants EAR05-38334 and CMMI09-19584), the Yosemite Conservancy through the Hawaii-Pacific Islands Cooperative Ecosystems Studies Unit (agreement J8834110001), and JPL (agreement 1290138). The digital topographic data used for this paper were collected by the National Center for Airborne Laser Mapping and are archived at the University of California at Berkeley. I gratefully acknowledge Taylor Perron, Paul Wessel, Fred Duennebier, Greg Stock, and Louis Martel for technical help, Kelly Mitchell for helpful discussions, Robert Anderson and Michael Bevis for their constructive critical reviews, and Ruth Harris for editorial aid. This is SOEST contribution 8493.

[23] The Editor thanks Michael Bevis and Robert Anderson for their assistance in evaluating this paper.

References

Bahat, D., K. Grossenbacher, and K. Karasaki (1999), Mechanism of exfoliation joint formation in granitic rocks, Yosemite National Park, *J. Struct. Geol.*, *21*, 85–96, doi:10.1016/S0191-8141(98)00069-8.

Bazant, Z. P. (1996), Is no-tension design of concrete or rock structures always safe?—Fracture analysis, *J. Struct. Eng.*, *122*, 2–10, doi:10.1061/(ASCE)0733-9445(1996)122:1(2).

Borchers, J. W. (1996), Ground-water resources and water-supply alternatives in the Wawona area of Yosemite National Park, California, pp., *U.S. Geol. Surv. Water Resour. Invest. Rep., 95-4229*.

Bradley, W. C. (1963), Large-scale exfoliation in massive sandstones of the Colorado Plateau, *Geol. Soc. Am. Bull.*, *74*, 519–528, doi:10.1130/0016-7606(1963)74[519:LEIMSO]2.0.CO;2.

Cadman, J. (1970), The origin of exfoliation joints in granitic rocks, Ph.D. dissertation, Dep. of Civ. Eng., Univ. of Calif., Berkeley.

Chigira, M. (2001), Micro-sheeting of granite and its relationship with landsliding after the heavy rainstorm in June, 1999, Hiroshima Prefecture, Japan, *Eng. Geol.*, *59*, 219–231, doi:10.1016/S0013-7952(00)00075-2.

Dale, T. N. (1923), The commercial granites of New England, *U.S. Geol. Surv. Bull.*, *738*.

Gauss, K. F. (2005), *General Investigations of Curved Surfaces*, Dover, Mineola, N. Y.

Gilbert, G. K. (1904), Dome and dome structures of the High Sierra, *Geol. Soc. Am. Bull.*, *15*, 29–36.

Gillespie, A. R., and P. H. Zehfuss (2004), Glaciations of the Sierra Nevada, California, USA, in *Quaternary Glaciations: Extent and Chronology—Part II: North America*, edited by J. Ehlers and P. L. Gibbard, pp. 51–62, Elsevier, Amsterdam.

He, M. Y., A. G. Evans, and J. W. Hutchinson (1998), Effects of morphology on the decohesion of compressed thin films, *Mater. Sci. Eng. A*, *245*, 168–181, doi:10.1016/S0921-5093(97)00848-4.

Hermanns, R. L., and M. R. Strecker (1999), Structural and lithological controls on large Quaternary rock avalanches (sturzstroms) in arid northwestern Argentina, *Geol. Soc. Am. Bull.*, *111*, 934–948, doi:10.1130/0016-7606(1999)111<0934:SALCOL>2.3.CO;2.

Hickman, S., J. Svitek, J. Borchers, and E. Scholz (1993), In-situ stress measurements at Wawona, Yosemite National Park, California, *Eos Trans. AGU*, *74*, 581.

Holzhausen, G. R. (1977), Sheet structure in rock and some related problems in rock mechanics, Ph.D. dissertation, Dep. of Appl. Earth Sci., Stanford Univ., Stanford, Calif.

Holzhausen, G. R. (1989), Origin of sheet structure. 1. Morphology and boundary conditions, *Eng. Geol.*, *27*, 225–278, doi:10.1016/0013-7952(89)90035-5.

Jahns, R. H. (1943), Sheet structure in granites, its origin and use as a measure of glacial erosion in New England, *J. Geol.*, *51*, 71–98, doi:10.1086/625130.

LeGrand, H. E. (1949), Sheet structure, a major factor in the occurrence of ground water in the granites of Georgia, *Econ. Geol.*, *44*, 110–118, doi:10.2113/gsecongeo.44.2.110.

Malvern, L. E. (1969), *Introduction to the Mechanics of a Continuous Medium*, Prentice Hall, Upper Saddle River, N. J.

Martel, S. J. (2006), Effect of topographic curvature on near-surface stresses and application to sheeting joints, *Geophys. Res. Lett.*, *33*, L01308, doi:10.1029/2005GL024710.

Matthes, F. E. (1930), Geologic history of the Yosemite Valley, *U.S. Geol. Surv. Prof. Pap.*, *160*.

Nemat-Nasser, S., and H. Horii (1982), Compression-induced nonplanar crack extension with application to splitting, exfoliation, and rockburst, *J. Geophys. Res.*, *87*, 6805–6821, doi:10.1029/JB087iB08p06805.

Niles, W. H. (1871), Peculiar phenomena observed in quarrying, *Proc. Boston Soc. Nat. Hist.*, *14*, 4.

Perron, J. T., J. W. Kirchner, and W. E. Dietrich (2008), Spectral signatures of characteristic spatial scales and non-fractal structure in landscapes, *J. Geophys. Res.*, *113*, F04003, doi:10.1029/2007JF000866.

Pollard, D. D., and P. Segall (1987), *Fracture Mechanics of Rock*, edited by B. K. Atkinson, pp. 277–349, Academic, London.

Savage, W. Z., and H. S. Swolfs (1986), Tectonic and gravitational stress in long symmetric ridges and valleys, *J. Geophys. Res.*, *91*, 3677–3685, doi:10.1029/JB091iB03p03677.

Terzaghi, K. (1962), Dam foundation on sheeted granite, *Geotechnique*, *12*, 199–208, doi:10.1680/geot.1962.12.3.199.

Thornbury, W. D. (1954), *Principles of Geomorphology*, Wiley, New York.

Trainer, F. W. (1988), Hydrogeology of the plutonic and metamorphic rocks, in *The Geology of North America*, vol. O2, *Hydrogeology*, edited by W. Back, J. S. Rosenshein and P. R. Seaber, pp. 367–380, Geol. Soc. of Am., Boulder, Colo.

Twidale, C. R. (1973), On the origin of sheet jointing, *Rock Mech. Rock Eng.*, *5*, 163–187.

Twidale, C. R., and J. A. Bourne (2000), Rock bursts and associated neotectonic forms at Minnipa Hill, northwestern Eyre Peninsula, South Australia, *Environ. Eng. Geosci.*, *6*, 129–140.

Vidal Romaní, J. R., and C. R. Twidale (1999), Sheet fractures, other stress forms and some engineering implications, *Geomorphology*, *31*, 13–27, doi:10.1016/S0169-555X(99)00070-7.

Wieczorek, G. F., and J. B. Snyder (1999), Rock falls from Glacier Point above Camp Curry, Yosemite National Park, California, *U.S. Geol. Surv. Open File Rep., 99-385*.

S. J. Martel, Department of Geology and Geophysics, University of Hawaii, 1680 East-West Rd., Honolulu, HI 96822, USA. (smartel@hawaii.edu)